CeO_2-Promoted Highly Active Catalyst, $NiSO_4/CeO_2$-ZrO_2 for Ethylene Dimerization

Young Il Pae,[†] Dong Cheol Shin, and Jong Rack Sohn[*]

Department of Applied Chemistry, Engineering College, Kyungpook National University, Daegu 702-701, Korea
[*]E-mail: jrsohn@knu.ac.kr
[†]Department of Chemistry, University of Ulsan, Ulsan 680-746, Korea
Received June 16, 2006

The $NiSO_4/CeO_2$-ZrO_2 catalysts containing different nickel sulfate and CeO_2 contents were prepared by the impregnation method, where support, CeO_2-ZrO_2 was prepared by the coprecipitation method using a mixed aqueous solution of zirconium oxychloride and cerium nitrate solution followed by adding an aqueous ammonia solution. No diffraction line of nickel sulfate was observed up to 20 wt %, indicating good dispersion of nickel sulfate on the surface of CeO_2-ZrO_2. The addition of nickel sulfate (or CeO_2) to ZrO_2 shifted the phase transition of ZrO_2 from amorphous to tetragonal to higher temperatures because of the interaction between nickel sulfate (or CeO_2) and ZrO_2. A catalyst (10-$NiSO_4$/1-CeO_2-ZrO_2) containing 10 wt % $NiSO_4$ and 1 mole % CeO_2, and calcined at 600 °C exhibited a maximum catalytic activity for ethylene dimerization. The catalytic activities were correlated with the acidity of catalysts measured by the ammonia chemisorption method. The role of CeO_2 was to form a thermally stable solid solution with zirconia and consequently to give high surface area, thermal stability and acidity of the sample.

Key Words : $NiSO_4/CeO_2$-ZrO_2 catalyst, Promoting effect of CeO_2, Acidic properties, Ethylene dimerization

Introduction

Solid acids have found widespread applications in many catalytic reactions concerning hydrocarbons, such as alkane or alkene isomerization, oligomerization, alkylation, and cracking. Liquid superacids based on HF, which are efficient and selective at room temperature, are not suitable for industrial processes due to separation problems tied with environmental regulations.[1] Many catalysts were reported in the literature including $AlCl_3$ with additives like $SbCl_3$ and HCl, chlorinated alumina, transition metal-exchanged zeolites, heteropoly acids and some bifunctional catalysts.[2] Most of these catalysts suffer from different draw backs such as high working temperature, continuous supply of chlorine and a high hydrogen pressure. Conventional industrial acid catalysts, such as sulfuric acid, $AlCl_3$, and BF_3, have unavoidable drawbacks because of their severe corrosivity and high susceptibility to water. Thus the search for environmentally benign heterogeneous catalysts has driven the worldwide research of new materials as a substitute for current liquid acids and halogen-based solid acids. Among them sulfated oxides, such as sulfated zirconia, titania, and iron oxide exhibiting high thermostability, superacidic property, and high catalytic activity, have evoked increasing interest.[3-5] The strong acidity of zircona-supported sulfate has attracted much attention because of its ability to catalyze many reactions such as cracking, alkylation, and isomerization.

In recent years, promoted zirconia catalysts have gained much attention for isomerization reactions due to their superacidity, non-toxicity and a high activity at low temperatures.[3,6] Sulfated zirconia incorporating Fe and Mn has been shown to be highly active for butane isomerization, catalyzing the reaction even at room temperature.[7,8] Such promotion in activity of catalyst has been confirmed by several other research groups.[8-10] Coelho *et al.*[11] have discovered that the addition of Ni to sulfated zirconia results in an activity enhancement comparable to that caused by the addition of Fe and Mn. It has been reported by several workers that the addition of platinum to zirconia modified by sulfate ions enhances catalytic activity in the skeletal isomerization of alkanes without deactivation when the reaction is carried out in the presence of hydrogen.[12,13] The high catalytic activity and small deactivation can be explained by both the elimination of the coke by hydrogenation and hydrogenolysis, and the formation of Brönsted acid sites from H_2 on the catalysts.[12] Recently, it has been found that a main group element Al can also promote the catalytic activity and stability of sulfated zirconia for *n*-butane isomerization.[14,15]

Many metal sulfates generate fairly large amounts of acid sites of moderate or strong strength on their surfaces when they are calcined at 400-700 °C.[4,16] The acidic property of metal sulfate often gives high selectivity for diversified reactions such as hydration, polymerization, alkylation, cracking, and isomerization. Structural and physicochemical properties of supported metal sulfates are considered to be in different states compared with bulk metal sulfates because of their interaction with supports.[17-19] Heterogeneous catalysts for the dimerization and oligomerization of olefins, consisting mainly of nickel compounds supported on oxides, have been known for many years. A considerable number of papers have dealt with the nickel-containing catalysts for ethylene dimerization.[17,20-28] One of the remarkable features of this catalyst system is its activity in relation to a series of *n*-olefins. In contrast to usual acid-type catalysts, nickel

oxide on silica or silica-alumina shows a higher activity for a lower olefin dimerization, particularly for ethylene.[20-25,29] It has been suggested that the active site for dimerization is formed by an interaction of a low-valent nickel ion with an acid site.[17,30] It has been reported that the dimerization activities of such catalysts are related to the acidic property of surface and low valent nickel ions. In our previous work,[31] it has been shown that $NiSO_4$ supported on ZrO_2 is very active for ethylene dimerization. It came to our attention that nickel sulfate catalysts supported on ZrO_2 promoted with CeO_2 have not been reported up to now. In the present work, the promoting effect of CeO_2 on catalytic activity of $NiSO_4$ on ZrO_2 was studied as an extension of our study on ethylene dimerization.

Experimental

Catalyst Preparation. The CeO_2-ZrO_2 mixed oxide was prepared by a co-precipitation method using aqueous ammonia as the precipitation reagent. The coprecipitate of $Ce(OH)_3$-$Zr(OH)_4$ was obtained by adding aqueous ammonia slowly into a mixed aqueous solution of cerium(III) nitrate and zirconium oxychloride (Junsei Chemical Co.) at room temperature with stirring until the pH of the mother liquor reached about 8. Catalysts containing various nickel sulfate contents were prepared by the impregnation of $Ce(OH)_3$-$Zr(OH)_4$ powder with an aqueous solution of $NiSO_4$ followed by calcining at different temperatures for 1.5 h in air. This series of catalysts is denoted by the mol percentage of CeO_2 and the weight percentage of nickel sulfate. For example, 10-$NiSO_4$/5-CeO_2-ZrO_2 indicates the catalyst containing 5 mol % of CeO_2 and 10 wt % of $NiSO_4$.

Procedure. FTIR spectra were obtained in a heatable gas cell at room temperature using Mattson Model GL6030E spectrophotometer. The self-supporting catalyst wafers contained about 9 mg cm^{-2}. Prior to obtaining the spectra, each sample was heated under vacuum at 25-600 °C for 1 h. Catalysts were checked in order to determine the structure of the prepared catalysts by means of a Philips X'pert-APD X-ray diffractometer, employing Ni-filtered Cu K_α radiation. DSC measurements were performed by a PL-STA model 1500H apparatus in air, and the heating rate was 5 °C per minute. For each experiment 10-15 mg of sample was used.

The specific surface area was determined by applying the BET method to the adsorption of N_2 at –196 °C. Chemisorption of ammonia was also employed as a measure of the acidity of catalysts. The amount of chemisorption was determined based on the irreversible adsorption of ammonia.[32-34]

The catalytic activity for ethylene dimerization was determined at 20 °C using a conventional static system following the pressure change from an initial pressure of 290 Torr. A fresh catalyst sample of 0.2 g was used for every run and the catalytic activity was calculated as the amount of ethylene consumed in the initial 5 min. Reaction products were analyzed by gas chromatograph with a VZ-7 column at room temperature.

Results and Discussion

Infrared Spectra. The infrared spectra of 10-$NiSO_4$/1-CeO_2-ZrO_2 (KBr disc) calcined at different temperatures (400-800 °C) are given in Figure 1. The catalyst calcined up to 700 °C showed infrared absorption bands at 1239, 1183, 1089 and 985 cm^{-1} which are assigned to bidentate sulfate ion coordinated to the metal such as Zr^{4+} or Ce^{4+}.[18,19] The band at 1625 cm^{-1} is assigned to the deformation vibration mode of the adsorbed water. For 10-$NiSO_4$/1-CeO_2-ZrO_2 calcined at 700 °C, the band intensities of sulfate ion decreased because of the partial decomposition of sulfate ion. However, for the sample calcined at 800 °C infrared bands by the sulfate ion disappeared completely due to the decomposition of sulfate ion.

In general, for the metal oxides modified with sulfate ion followed by evacuation above 400 °C, a strong band[35,36] assigned to S=O stretching frequency is observed at 1390-1370 cm^{-1}. In a separate experiment infrared spectrum of self-supported 10-$NiSO_4$/1-CeO_2-ZrO_2 after evacuation at 500 °C for 1 h was examined. As shown in Figure 1, an intense band at 1391 cm^{-1} accompanied by broad and intense bands below 1250 cm^{-1} was observed due to the overlapping of the CeO_2 and ZrO_2 skeletal vibration, indicating the presence of different adsorbed species depending on the treatment conditions of the sulfated sample.[19,37]

Crystalline Structures of Catalysts. The crystalline structures of ZrO_2 and 5-CeO_2-ZrO_2 calcined in air at different temperatures for 1.5 h were examined. For pure ZrO_2, ZrO_2 was amorphous to X-ray diffraction up to 300 °C, with a two-phase mixture of the tetragonal and monoclinic forms at 400-700 °C and a monoclinic form at 800 °C (This figure is not shown here). Three crystal structures of ZrO_2, tetragonal, monoclinic and cubic phases have been reported.[38,39] How-

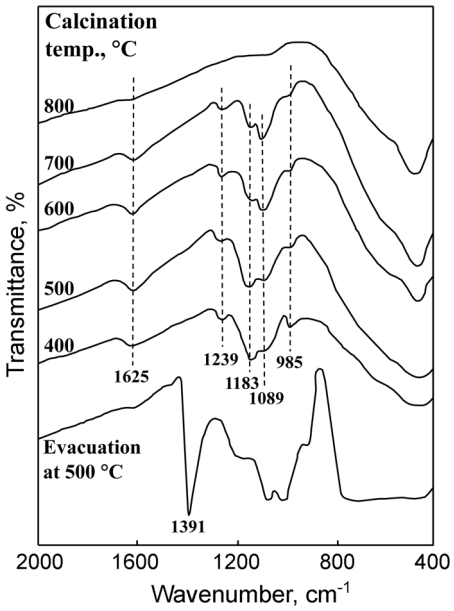

Figure 1. Infrared spectra of 10-$NiSO_4$/1-CeO_2-ZrO_2 calcined at different temperatures for 1.5 h.

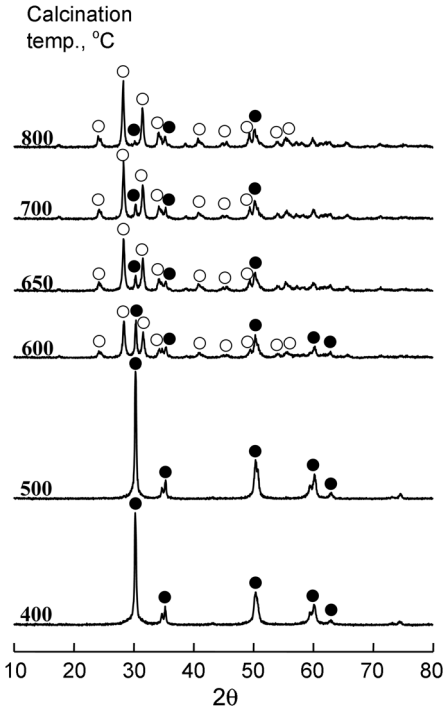

Figure 2. X-ray diffraction patterns of 5-CeO_2-ZrO_2 calcined at different temperatures for 1.5 h: (●), tetragonal phase of ZrO_2; (○), monoclinic phase of ZrO_2.

ever, in the case of 5-CeO_2-ZrO_2 promoted with CeO_2, the crystalline structures of the samples were different from that of pure ZrO_2. For the 5-CeO_2-ZrO_2, as shown in Figure 2, ZrO_2 was tetragonal phase up to 500 °C, with a two-phase mixture of the tetragonal and monoclinic forms at 600-800 °C. The transition temperature of ZrO_2 from tetragonal to monoclinic phase was higher by 200 °C than of pure ZrO_2. It is assumed that the interaction between CeO_2 and ZrO_2 hinders the transition of ZrO_2 from tetragonal to monoclinic phase.[33,40] It is known that the role of CeO_2 in the catalysts is to form a thermally stable solid solution with ZrO_2.[41,42] The presence of cerium oxide strongly influences the development of textural properties with temperature.

The crystalline structures of 10-$NiSO_4$/5-CeO_2-ZrO_2 calcined in air at different temperatures for 1.5 h were checked by X-ray diffraction. In the case of supported nickel sulfate catalysts the crystalline structures of the samples were different from structure of the ZrO_2, support. For the 10-$NiSO_4$/5-CeO_2-ZrO_2 calcined at different temperatures, as shown in Figure 3, ZrO_2 is amorphous up to 500 °C. In other words, the transition temperature from amorphous to tetragonal phase was higher by 250 °C than that of pure ZrO_2.[31] X-ray diffraction data indicated only tetragonal phase of ZrO_2 at 600-800 °C, without detection of orthorhombic $NiSO_4$ phase. However, the amount of tetragonal ZrO_2 phase increased with increasing the calcination temperature, as shown in Figure 3. It is assumed that the interaction between $NiSO_4$ (or CeO_2) and ZrO_2 hinders the phase transition of ZrO_2 from amorphous to tetragonal.[19]

The XRD patterns of $NiSO_4$/5-CeO_2-ZrO_2 containing different nickel sulfate contents and calcined at 600 °C for 1.5 h are shown in Figure 4. XRD data indicated only tetragonal phase of ZrO_2 at the region of 5-20 wt % of nickel sulfate, indicating good dispersion of $NiSO_4$ on the surface of 5-

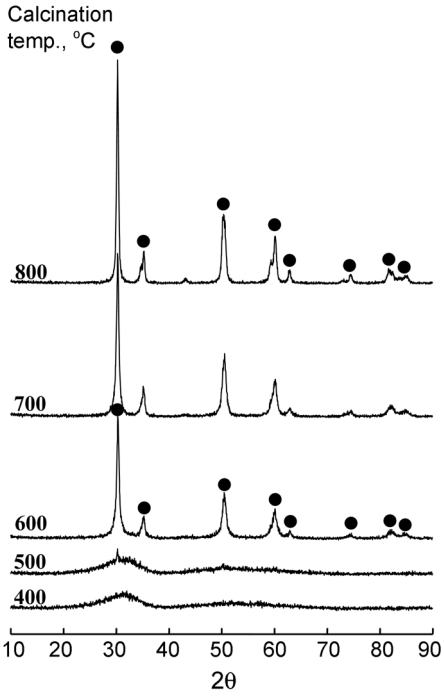

Figure 3. X-ray diffraction patterns of 10-$NiSO_4$/5-CeO_2-ZrO_2 as a function of calcination temperature: (●), tetragonal phase of ZrO_2.

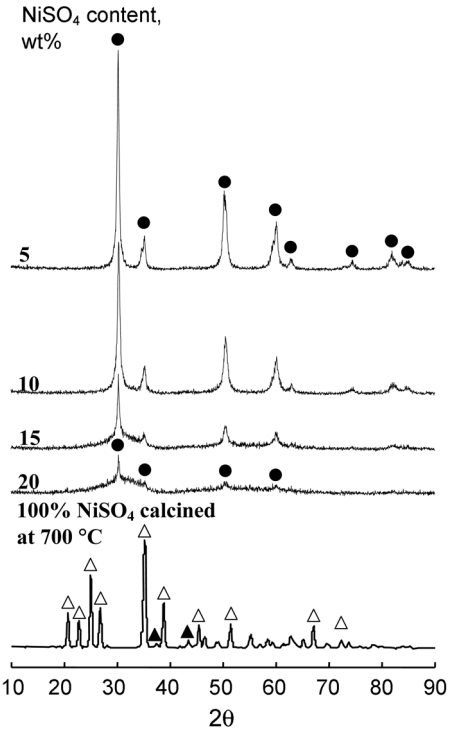

Figure 4. X-ray diffraction patterns of $NiSO_4$/5-CeO_2-ZrO_2 having different $NiSO_4$ contents and calcined 600 °C for 1.5 h: (●), tetragonal phase of ZrO_2; (△), orthorhombic phase of $NiSO_4$; (▲), cubic phase of NiO.

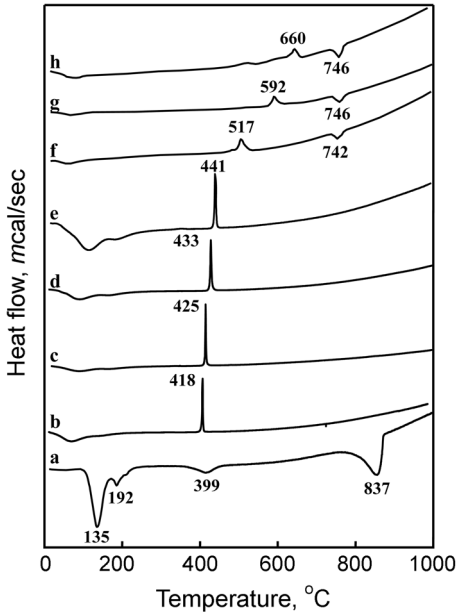

Figure 5. DSC curves of CeO_2-ZrO_2 and $NiSO_4$/CeO_2-ZrO_2 precursors having different CeO_2 and $NiSO_4$ contents: (a) $NiSO_4 \cdot 6H_2O$, (b) ZrO_2, (c) 1-CeO_2-ZrO_2, (d) 3-CeO_2-ZrO_2, (e) 5-CeO_2-ZrO_2, (f) 5-$NiSO_4$/1-CeO_2-ZrO_2, (g) 10-$NiSO_4$/1-CeO_2-ZrO_2, (h) 15-$NiSO_4$/1-CeO_2-ZrO_2.

CeO_2-ZrO_2. However, the higher the content of $NiSO_4$, the lower is the amount of tetragonal ZrO_2 phase, because the interaction between nickel sulfate and ZrO_2 hinders the phase transition of ZrO_2 from amorphous to tetragonal in proportion to the nickel sulfate content.[19] As shown in Figure 4, for pure $NiSO_4$ calcined at 700 °C, the cubic phase of NiO besides orthorhombic phase of $NiSO_4$ was observed due to the decomposition of $NiSO_4$.

Thermal Analysis. The X-ray diffraction patterns in Figures 2-4 clearly showed that the structure of $NiSO_4$/CeO_2-ZrO_2 was different depending on the calcined temperature. To examine the thermal properties of precursors of $NiSO_4$/CeO_2-ZrO_2 samples more clearly, their thermal analysis has been carried out and the results are illustrated in Figure 5. For pure ZrO_2, the DSC curve shows a broad endothermic peak below 200 °C due to water elimination, and a sharp exothermic peak at 418 °C due to the ZrO_2 crystallization.[19] However, it is of interest to see the influence of CeO_2 on the crystallization of ZrO_2 from amorphous to tetragonal phase. As Figure 5 shows, the exothermic peak due to the crystallization appears at 418 °C for pure ZrO_2, while for CeO_2-ZrO_2 samples it is shifted to higher temperatures due to the interaction between CeO_2 and ZrO_2. The shift increases with increasing CeO_2 content. Consequently, the exothermic peaks appear at 425 °C for 1-CeO_2-ZrO_2, 433 °C for 3-CeO_2-ZrO_2, and 441 °C for 5-CeO_2-ZrO_2.

However, for $NiSO_4$/1-CeO_2-ZrO_2 samples containing different $NiSO_4$ contents, the DSC patterns are somewhat different from that of CeO_2-ZrO_2. As shown in Figure 5, the exothermic peak for $NiSO_4$/1-CeO_2-ZrO_2 due to the crystallization of ZrO_2 is shifted to more higher temperatures and the shape of peak become broad compared with that for 1-CeO_2-ZrO_2 without $NiSO_4$, indicating that there is an interaction between $NiSO_4$ and ZrO_2 in addition to the interaction between CeO_2 and ZrO_2. The exothermic peaks appear at 517 °C for 5-$NiSO_4$/1-CeO_2-ZrO_2, 592 °C for 10-$NiSO_4$/1-CeO_2-ZrO_2, and 660 °C for 15-$NiSO_4$/1-CeO_2-ZrO_2. The endothermic peaks for $NiSO_4$/1-CeO_2-ZrO_2 samples in the region of 742-746 °C are due to the evolution of SO_3 decomposed from sulfate species bonded to the surface of CeO_2-ZrO_2. For pure $NiSO_4 \cdot 6H_2O$, the DSC curve shows three endothermic peaks below 400 °C due to water elimination, indicating that the dehydration of $NiSO_4 \cdot 6H_2O$ occurs in three steps. The endothermic peak around 837 °C is due to the evolution of SO_3 decomposed from nickel sulfate.[14,43] Decomposition of nickel sulfate is known to begin at 700 °C.[44]

Table 1. Surface area and acidity of $NiSO_4$/1-CeO_2-ZrO_2 catalysts containing different $NiSO_4$ contents and calcined at 600 °C for 1.5 h

$NiSO_4$ content (mol%)	Surface area (m^2/g)	Acidity (μmol/g)
0	32	40
5	67	118
10	83	184
15	40	167
20	35	136

Surface Properties

Specific Surface Area and Acidity: The specific surface areas of samples calcined at 600 °C for 1.5 h are listed in Table 1. The presence of nickel sulfate and CeO_2 influences the surface area in comparison with the pure ZrO_2. Specific surface areas of $NiSO_4$/1-CeO_2-ZrO_2 samples are larger than that of 1-CeO_2-ZrO_2 calcined at the same temperature, showing that surface area increases gradually with increasing nickel sulfate loading up to 10 wt%. It seems likely that the interaction between nickel sulfate (or CeO_2) and ZrO_2 prevents catalysts from crystallizing.[40] The decrease of surface area for $NiSO_4$/5-CeO_2-ZrO_2 samples containing $NiSO_4$ above 10 wt % is due to the block of ZrO_2 pore by the increased $NiSO_4$ loading. The acidity of catalysts calcined at 600 °C, as determined by the amount of NH_3 irreversibly adsorbed at 230 °C,[32-34] is also listed in Table 1. The variation of acidity runs parallel to the change of surface area. The acidity increases with increasing nickel sulfate content up to 10 wt % of $NiSO_4$. The acidity is correlated with the catalytic activity for ethylene dimerization discussed below.

Effect of CeO_2 Addition on Surface Properties: We examined the effect of CeO_2 addition on the surface area and acidity of $NiSO_4$/CeO_2-ZrO_2 samples. The specific surface areas and acidity of 10-$NiSO_4$/CeO_2-ZrO_2 catalysts containing different CeO_2 contents and calcined at 600 °C are listed in Table 2. Both surface area and acidity exhibited maxima upon the addition of 1 mol% (CeO_2), indicating the promoting effect of CeO_2 on the catalytic activities for ethylene dimerization described later.

Infrared spectroscopic studies of ammonia adsorbed on solid surfaces have made it possible to distinguish between

Table 2. Surface area and acidity of 10-$NiSO_4/CeO_2$-ZrO_2 catalysts containing different CeO_2 contents and calcined at 600 °C for 1.5 h

CeO_2 content (mol%)	Surface area (m^2/g)	Acidity (μmol/g)
0	45	142
1	83	184
3	77	172
5	73	169
10	44	154

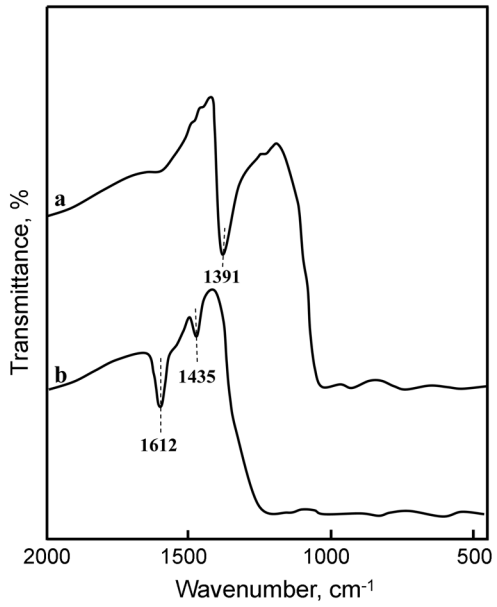

Figure 6. Infrared spectra of NH_3 adsorbed on 10-$NiSO_4$/1-CeO_2-ZrO_2: (a) background of 10-$NiSO_4$/1-CeO_2-ZrO_2 after evacuation at 500 °C for 1 h, (b) NH_3 adsorbed on (a), where gas was evacuated at 230 °C for 1 h.

Brönsted and Lewis acid sites.[5,43,45] Figure 6 shows the infrared spectra of ammonia adsorbed on 10-$NiSO_4$/1-CeO_2-ZrO_2 samples evacuated at 500 °C for 1 h. For 10-$NiSO_4$/1-CeO_2-ZrO_2 the band at 1435 cm^{-1} is the characteristic peak of ammonium ion, which is formed on the Brönsted acid sites and the absorption peak at 1612 cm^{-1} is contributed by ammonia coordinately bonded to Lewis acid sites,[5,43,45] indicating the presence of both Brönsted and Lewis acid sites on the surface of 10-$NiSO_4$/1-CeO_2-ZrO_2 sample. Other samples having different nickel sulfate contents also showed the presence of both Lewis and Brönsted acids. As Figure 6(a) shows, the intense band at 1391 cm^{-1} after evacuation at 500 °C is assigned to the asymmetric stretching vibration of S=O bonds having a high double bond nature.[36,43] However, the drastic shift of the infrared band from 1391 cm^{-1} to a lower wavenumber (not shown due to the overlaps of skeletal vibration bands of CeO_2-ZrO_2) after ammonia adsorption [Figure 6(b)] indicates a strong interaction between an adsorbed ammonia molecule and the surface complex. Namely, the surface sulfur compound in the highly acidic catalysts has a strong tendency to reduce the bond order of S=O from a highly covalent double-bond character to a lesser double-bond character when a basic ammonia molecule is adsorbed on the catalysts.[36,43]

Acids stronger than $H_o \leq -11.93$, which corresponds to the acid strength of 100% H_2SO_4, are superacids.[3,4,36,46] The strong ability of the sulfur complex to accommodate electrons from a basic molecule such as ammonia is a driving force to generate superacidic properties.[4,36,43] $NiSO_4/CeO_2$-ZrO_2 samples after evacuation at 500 °C for 1 h was also examined by color change method, using Hammet indicator in sulfuryl chloride.[33,47] The samples were estimated to have $H_o \leq -14.5$, indicating the formation of superacidic sites. Consequently, $NiSO_4$/1-CeO_2-ZrO_2 catalysts would be solid superacids, in analogy with the case of metal oxides modified with a sulfate group.[5,32,36,48] This superacidic property is attributable to the double bond nature of the S=O in the complex formed by the interaction between $NiSO_4$ and 1-CeO_2-ZrO_2.[3,17,36,48] In other words, the acid strength of $NiSO_4/CeO_2$-ZrO_2 becomes stronger by the inductive effect of S=O in the complex.

Catalytic Activities for Ethylene Dimerization

Effect of Calcination Temperature on Catalytic Activity: The catalytic activities of 10-$NiSO_4$/1-CeO_2-ZrO_2 were tested as a function of calcination temperature. The results are shown in Figure 7, where catalysts were evacuated at 500 °C for 1 h. The activities increased with the calcination temperature, reaching a maximum at 600 °C, and then the activities decreased. The decrease of catalytic activity after calcination above 600 °C seems to be due to the decomposition of sulfate ion bonded to 1-CeO_2-ZrO_2 at high calcination temperatures. Especially, 10-$NiSO_4$/1-CeO_2-ZrO_2 calcined at 800 °C exhibited absolutely no catalytic activity after initial adsorption of ethylene on the surface of catalyst, because sulfate species bonded to 1-CeO_2-ZrO_2 decomposed completely under the calcination condition of 800 °C, as shown in Figure 1. Thus, hereafter, emphasis is placed only on the

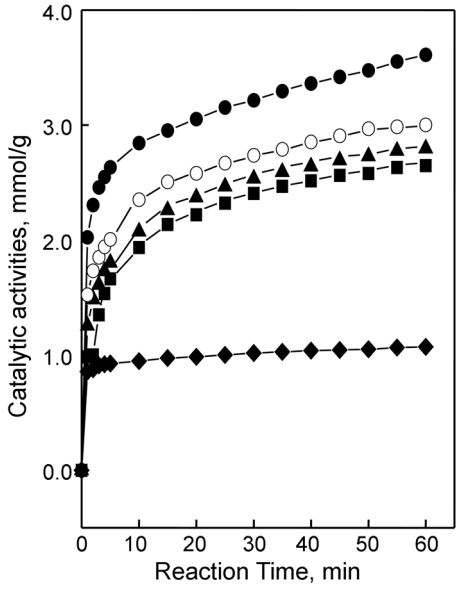

Figure 7. Catalytic activities of 10-$NiSO_4$/1-CeO_2-ZrO_2 as a function of calcination temperature: (●), 600 °C; (○), 700 °C; (▲), 500 °C; (■), 400 °C, (◆), 800 °C.

$NiSO_4/CeO_2$-ZrO_2 samples calcined at 600 °C.

It was found that over 10-$NiSO_4/CeO_2$-ZrO_2, ethylene was continuously consumed, as shown by the results presented in Figure 7. Over all catalysts, ethylene was selectively dimerized to *n*-butenes. However, a small amount of hexenes from the phase adsorbed on the catalyst surface was detected. In the composition of *n*-butenes analyzed by gas chromatography, 1-butene was found to predominate exclusively at the initial reaction time, as compared with cis-butene and trans-butene. This is because the initial product of ethylene dimerization is 1-butene.[5,17,23] Therefore, the initially produced 1-butene is also isomerized to 2-butene during the reaction time.[5,43,49,50]

Promoting Effect of CeO_2 on Catalytic Activity: The catalytic activity of 10-$NiSO_4/CeO_2$-ZrO_2 as a function of CeO_2 content for the reaction of ethylene dimerization was examined, where the catalysts were evacuated at 500 °C for 1 h before reaction; the results are shown in the Figure 8. The catalytic activity increased with increasing the CeO_2 content, reaching a maximum at 1 mol %.

Considering the experimental results of Table 2, and Figure 8, it seems likely that the catalytic activity for ethylene dimerization closely relates to the change of surface area and the acidity of catalysts. CeO_2-promoted catalysts could be related to a strong interaction between CeO_2 and ZrO_2. Since the promoting effect of CeO_2 is related to an increase in number of surface acidic sites, it would be of interest to examine various factors influencing the enhancement of these surface acidic sites.

In general, it is known that a small amount of rare-earth solutes in nanophase zirconia powders can stabilize the tetragonal and cubic phases over a wide range of temperatures.[51] Considering the experimental results of Table 2 and Figure 8, it seems likely that the catalytic activities for ethylene dimerization closely relates to the change of acidity of catalysts. As listed in Table 2, the total acid sites of 10-$NiSO_4$/1-CeO_2-ZrO_2 and 10-$NiSO_4/ZrO_2$ are 184 μmol/g and 142 μmol/g, respectively, showing that the number of acid sites for the catalyst doped with CeO_2 is greater than that for undoped catalyst. This high surface area and acidity are due to the CeO_2 doping effect which makes zirconia tetragonal phase as confirmed by XRD, as shown in Figures 3 and 4. This is consistent with the results reported by Roh *et al*. over Ce-doped Ni/Ce-ZrO_2.[52] The doping effect of CeO_2 is related to an increase in number of surface acidic sites.

The formation of solid solution, CeO_2-ZrO_2 results in an increase in the thermal stability of the surface sulfate species and consequently the acidity of CeO_2-doped catalyst is increased. In fact, to examine the thermal stability of the surface sulfate species DSC measurements were carried out.[53] The endothermic peak due to the evolution of SO_3 decomposed from sulfate species bonded to the surface of ZrO_2 appeared at 718 °C, while that from sulfate species bonded to the surface of CeO_2-doped ZrO_2 appeared at 742-746 °C, as shown in Figure 5. Such a temperature difference has been attributed to the stabilizing effect of the CeO_2 dopant on the sulfate species. The CeO_2-ZrO_2 solid solution leads to an increase in the thermal stability of the surface sulfate species and consequently the acidity of the catalysts is increased.

Catalytic Activity as a Function of $NiSO_4$ Content: The catalytic activity of $NiSO_4$/1-CeO_2-ZrO_2 containing different $NiSO_4$ contents was examined; the results are shown as a function of $NiSO_4$ content in Figure 9. Catalysts were evacuated at 500 for 1 h before each reaction. The catalytic activity gives a maximum at 10 wt % of $NiSO_4$. This seems to be correlated to the specific surface area and to the acidity

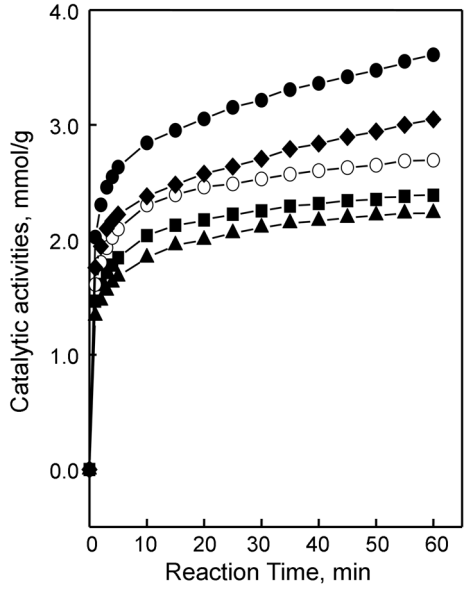

Figure 8. Catalytic activities of 10-$NiSO_4/CeO_2$-ZrO_2 as a function of CeO_2: (●), 10-$NiSO_4$/1-CeO_2-ZrO_2; (◆), 10-$NiSO_4$/3-CeO_2-ZrO_2; (○), 10-$NiSO_4/ZrO_2$; (■), 10-$NiSO_4$/5-CeO_2-ZrO_2; (▲), 10-$NiSO_4$/10-CeO_2-ZrO_2.

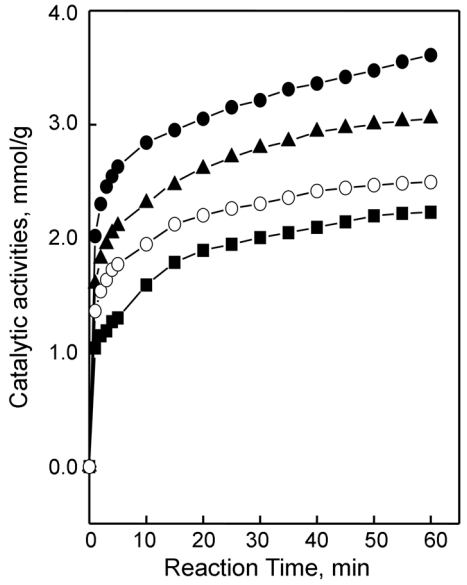

Figure 9. Catalytic activities of $NiSO_4$/1-CeO_2-ZrO_2 as a function of $NiSO_4$ content: (●), 10-$NiSO_4$/1-CeO_2-ZrO_2; (▲), 15-$NiSO_4$/1- CeO_2-ZrO_2; (○), 20-$NiSO_4$/1- CeO_2-ZrO_2; (■), 5-$NiSO_4$/1-CeO_2-ZrO_2.

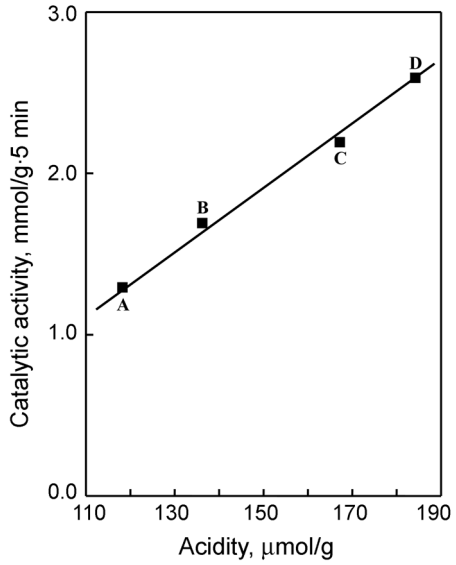

Figure 10. Correlationship between catalytic activity for ethylene dimerization and acidity: (A), 5-$NiSO_4$/1-CeO_2-ZrO_2; (B), 20-$NiSO_4$/1-CeO_2-ZrO_2; (C), 15-$NiSO_4$/1-CeO_2-ZrO_2; (D), 10-$NiSO_4$/1-CeO_2-ZrO_2.

of catalysts. The acidity of $NiSO_4$/1-CeO_2-ZrO_2 calcined at 600 °C was determined by the amount of NH_3 irreversibly adsorbed at 230 °C.[32-34] As listed in Tables 1, the BET surface area attained a maximum extent when the $NiSO_4$ content in the catalyst was 10 wt % and then showed a gradual decrease with increasing $NiSO_4$ content due to the block of ZrO_2 pore by the increased $NiSO_4$ loading. In view of Table 1 and Figure 9, the higher the acidity, the higher the catalytic activity. We plotted the catalytic activity against acidity; the results are shown in Figure 10. For $NiSO_4$/1-CeO_2-ZrO_2 both catalytic activity and acidity reached maxima at 10 wt% $NiSO_4$. Figure 10 shows a good correlation between the catalytic activity and the acidity. Good correlations have been found in many cases between the acidity and the catalytic activities of solid acids. For example, the rates of both the catalytic decomposition of cumene and the polymerization of propylene over SiO_2-Al_2O_3 and supported NiO catalysts were found to increase with increasing acid amount at strength $H_o \leq +3.3$.[54,55] The catalytic activity of nickel-containing catalysts in ethylene dimerization as well as in butene isomerization is closely correlated with the acidity of the catalyst.[17,23,28,56]

Conclusions

A series of catalysts, $NiSO_4/CeO_2$-ZrO_2 was prepared by the impregnation method using an aqueous solution of nickel sulfate. For $NiSO_4/CeO_2$-ZrO_2 sample, no diffraction line of nickel sulfate was observed up to 20 wt %, indicating good dispersion of nickel sulfate on the surface of CeO_2-ZrO_2. The addition of nickel sulfate (or CeO_2) to ZrO_2 shifted the phase transition of ZrO_2 from amorphous to tetragonal to higher temperatures because of the interaction between nickel sulfate (or CeO_2) and ZrO_2. 10-$NiSO_4/CeO_2$-ZrO_2 containing 10 wt% $NiSO_4$ and 1 mole % CeO_2, and calcined at 600 °C exhibited a maximum catalytic activity for ethylene dimerization. $NiSO_4/CeO_2$-ZrO_2 catalysts were very effective for ethylene dimerization even at room temperature, but CeO_2-ZrO_2 without $NiSO_4$ did not exhibit any catalytic activity at all. The catalytic activity was correlated with the acidity of catalysts measured by the ammonia chemisorption method. The addition of CeO_2 up to 1 mole % enhanced the acidity, surface area, thermal property, and catalytic activities of $NiSO_4/CeO_2$-ZrO_2 due to the formation of solid solution between CeO_2 and ZrO_2.

Acknowledgements. This work was supported by 2005 Research Fund of University of Ulsan. We wish to thank Korea Basic Science Institute (Daegu Branch) for the use of their X-ray diffractometer.

References

1. Olah, G. A.; Prakash, G. K. S.; Sommer, J. *Superacids*; Wiley-Interscience: New York, U. S. A., 1985; p 33.
2. Ono, Y. *Catal. Today* **2003**, *81*, 3.
3. Arata, K. *Adv. Catal*. **1990**, *37*, 165.
4. Tanabe, K.; Misono, M.; Ono, Y.; Hattori, H. *New Solid Acids and Bases*; Kodansha-Elsevier: Tokyo, 1989; p 185.
5. Sohn, J. R.; Lee, S. H. *Appl. Catal. A: Gen.* **2004**, *266*, 89.
6. Arata, K. *Appl. Catal. A: Gen.* **1996**, *146*, 3.
7. Hsu, C. Y.; Heimbuch, C. R.; Armes, C. T.; Gates, B. C. *J. Chem. Soc., Chem. Commun.* **1992**, 1645.
8. Adeeva, V.; de Haan, H. W.; Janchen, J.; Lei, G. D.; Schunemann, V.; van de Ven, L. J. M.; Sachtler, W. M. H.; van Santen, R. A. *J. Catal*. **1995**, *151*, 364.
9. Wan, K. T.; Khouw, C. B.; Davis, M. E. *J. Catal*. **1996**, *158*, 311.
10. Song, X.; Reddy, K. R.; Sayari, A. *J. Catal.* **1996**, *161*, 206.
11. Coelho, M. A.; Resasco, D. E.; Sikabwe, E. C.; White, R. L. *Catal. Lett.* **1995**, *32*, 253.
12. Ebitani, K.; Konishi, J.; Hattori, H. *J. Catal*. **1991**, *130*, 257.
13. Signoretto, M.; Pinna, F.; Strukul, G.; Chies, P.; Cerrato, G.; Ciero, S. D.; Morterra, C. *J. Catal*. **1997**, *167*, 522.
14. Hua, W.; Xia, Y.; Yue, Y.; Gao, Z. *J. Catal.* **2000**, *196*, 104.
15. Moreno, J. A.; Poncelet, G. *J. Catal*. **2001**, *203*, 153.
16. Arata, K.; Hino, M.; Yamagata, N. *Bull. Chem. Soc. Jpn*. **1990**, *63*, 244.
17. Sohn, J. R.; Park, W. C.; Kim, H. W. *J. Catal*. **2002**, *209*, 69.
18. Sohn, J. R.; Seo, D. H.; Lee, S. H. *J. Ind. Eng. Chem.* **2004**, *10*, 309.
19. Sohn, J. R.; Kim, J. G.; Kwon, T. D.; Park, E. H. *Langmuir* **2002**, *18*, 1666.
20. Urabe, K.; Koga, M.; Izumi, Y. *J. Chem. Soc., Chem. Commun*. **1989**, 807.
21. Bernardi, F.; Bottoni, A.; Rossi, I. *J. Am. Chem. Soc*. **1998**, *120*, 7770.
22. Sohn, J. R.; Ozaki, A. *J. Catal*. **1979**, *59*, 303.
23. Sohn, J. R.; Ozaki, A. *J. Catal*. **1980**, *61*, 29.
24. Wendt, G.; Fritsch, E.; Schöllner, R.; Siegel, H. Z. *Anorg. Allg. Chem*. **1980**, *467*, 51.
25. Sohn, J. R.; Shin, D. C. *J. Catal*. **1996**, *160*, 314.
26. Berndt, G. F.; Thomson, S. J.; Webb, G. J. *J. Chem. Soc. Faraday Trans. 1* **1983**, *79*, 195.
27. Herwijnen, T. V.; Doesburg, H. V.; Jong, D. V. *J. Catal*. **1973**, *28*, 391.
28. Sohn, J. R.; Han, J. S.; Kim, H. W.; Pae, Y. I. C. *Bull. Korean Chem. Soc*. **2005**, *26*, 755.
29. Wendt, G.; Hentschel, D.; Finster, J.; Schöllner, R. *J. Chem. Soc.*

Faraday Trans. 1 **1983**, *79*, 2013.
30. Kimura, K.; Ozaki, A. *J. Catal*. **1964**, *3*, 395.
31. Sohn, J. R.; Park, W. C. *Appl. Catal. A: Gen*. **2002**, *230*, 11.
32. Sohn, J. R.; Kim, H. W.; Park, M. Y.; Park, E. H.; Kim, J. T.; Park, S. E. *Appl. Catal. A: Gen.* **1995**, *128*, 127.
33. Sohn, J. R.; Cho, S. G.; Pae, Y. I.; Hayashi, S. *J. Catal*. **1996**, *159*, 170.
34. Sohn, J. R.; Choi, H. D.; Shin, D. C. *Bull. Korean Chem. Soc*. **2006**, *27*, 821.
35. Saur, O.; Bensitel, M.; Saad, A. B. M.; Lavalley, J. C.; Tripp, C. P.; Morrow, B. A. *J. Catal*. **1986**, *99*, 104.
36. Yamaguchi, T. *Appl. Catal.* **1990**, *61*, 1.
37. Morrow, B. A.; McFarlane, R. A.; Lion, M.; Lavalley, J. C. *J. Catal.* **1987**, *107*, 232.
38. Larsen, G.; Lotero, E.; Petkovic, L. M.; Shobe, D. S. *J. Catal*. **1997**, *169*, 67.
39. Afanasiev, P.; Geantot, C.; Breysse, M.; Coudurier, G.; Vedrine, J. C. *J. Chem. Soc., Faraday Trans.* **1994**, *190*, 193.
40. Sohn, J. R. *J. Ind. Eng. Chem.* **2004**, *10*, 1.
41. Dong, W.-S.; Roh, H.-S.; Jun, K.-W.; Park, S.-E.; Oh, Y.-S. *Appl. Catal. A: Gen*. **2002**, *226*, 63.
42. Loong, C.-K.; Ozawa, M. *J. Alloys Compd.* **2000**, *303-304*, 60.
43. Sohn, J. R.; Park ,W. C. *Appl. Catal. A: Gen.* **2003**, *239*, 269.
44. Siriwardane, R. V.; Poston, J. A. Jr.; Fisher, E. P.; Shen, M. S.; Miltz, A. L. *Appl. Surf. Sci.* **1999**, *152*, 219.
45. Satsuma, A.; Hattori, A.; Mizutani, K.; Furuta, A.; Miyamoto, A.; Hattori, T.; Murakami, Y. *J. Phys. Chem.* **1988**, *92*, 6052.
46. Olah, F. G. A.; Prakash, G. K. S.; Sommer, J. *Science* **1979**, *206*, 13.
47. Sohn, J. R.; Ryu, S. G.. *Langmuir* **1993**, *9*, 126.
48. Jin, T.; Yamaguchi, T.; Tananbe, K. *J. Phys. Chem*. **1986**, *90*, 4794.
49. Sohn, J. R.; Kim, H. J. *J. Catal.* **1986**, *101*, 428.
50. Sohn, J. R.; Lee, S. Y. *Appl. Catal. A: Gen.* **1997**, *164*, 127.
51. Loong, C.-K.; Richardson, Jr., J. W.; Ozawa, M. *J. Catal.* **1995**, *157*, 636.
52. Roh, H.-S.; Dong, W.-S.; Jun, K.-W.; Park, S.-E. *Chem. Lett.* **2001**, *30*, 88.
53. Sohn, J. R.; Lee, S. H.; Lim, J. S. *Catal. Today* **2006**, *116*, 143.
54. Tanabe, K. *Solid Acids and Bases*; Kodansha: Tokyo, 1970; p 103.
55. Sohn, J. R.; Han, J. S. J. *Ind. Eng. Chem.* **2005**, *11*, 439.
56. Sohn, J. R.; Lim, J. S. *Bull. Korean Chem. Soc.* **2005**, *26*, 1029.